

## Research Article

# Photocatalytic Reduction of CO<sub>2</sub> Using TiO<sub>2</sub>-Graphene Nanocomposites

Jinghua Liu,<sup>1</sup> Yinghua Niu,<sup>2,3</sup> Xiong He,<sup>1</sup> Jingyao Qi,<sup>4</sup> and Xin Li<sup>1,4</sup>

<sup>1</sup>Department of Chemistry, Harbin Institute of Technology, Harbin 150090, China

<sup>2</sup>School of Chemical Engineering and Technology, Harbin Institute of Technology, Harbin 150001, China

<sup>3</sup>School of Energy Science and Engineering, University of Electronic Science and Technology of China, Chengdu 611731, China

<sup>4</sup>State Key Lab of Urban Water Resources and Environment, Harbin Institute of Technology, Harbin 150090, China

Correspondence should be addressed to Jingyao Qi; [qjy\\_hit@hotmail.com](mailto:qjy_hit@hotmail.com) and Xin Li; [lixin@hit.edu.cn](mailto:lixin@hit.edu.cn)

Received 23 November 2015; Accepted 7 February 2016

Academic Editor: Godwin Ayoko

Copyright © 2016 Jinghua Liu et al. This is an open access article distributed under the Creative Commons Attribution License, which permits unrestricted use, distribution, and reproduction in any medium, provided the original work is properly cited.

TiO<sub>2</sub>-graphene (TiO<sub>2</sub>-RGO) nanocomposites were prepared *via* a simple chemical method by using graphene oxide (GO) and TiO<sub>2</sub> nanoparticles as starting materials. The morphologies and structural properties of the as-prepared composites were characterized by X-ray diffraction, Raman spectroscopy, N<sub>2</sub> adsorption-desorption measurements, and transmission electron microscopy. TiO<sub>2</sub>-RGO nanocomposites exhibited great photocatalytic activity toward reduction of CO<sub>2</sub> into CH<sub>4</sub> (2.10 μmol g<sup>-1</sup> h<sup>-1</sup>) and CH<sub>3</sub>OH (2.20 μmol g<sup>-1</sup> h<sup>-1</sup>), which is attributed to the synergistic effect between TiO<sub>2</sub> and graphene.

## 1. Introduction

The past few decades have witnessed the problem of global warming, which is dominantly caused by carbon dioxide emissions from fossil fuel consumption. Therefore, seeking for any alternative to minimize CO<sub>2</sub> emission has attracted increasing attention all over the world. The traditional method used to solve this problem is carbon capture and storage, but in fact this problem has never been solved radically because CO<sub>2</sub> does not convert into other substances [1]. The photocatalytic reduction of CO<sub>2</sub> into hydrocarbon fuels was found to be a prospective way [2].

TiO<sub>2</sub> is one of the most promising semiconductor materials used in the photocatalysis due to its excellent stability, nontoxicity, and low price [3]. Graphene, one atomic sp<sup>2</sup>-bonded planar carbon nanosheet, is a nearly ideal 2D nanoscale carbon material [4]. Due to the unique structure and excellent electronic, thermal, and mechanical properties, graphene is expected to be catalyst supports [5, 6]. The combination of graphene with TiO<sub>2</sub> can create composites with both the outstanding characters and functions of two components and lead to some additional novel properties.

Thus, graphene-based photocatalyst possesses numerous opportunities for the photocatalytic CO<sub>2</sub> reduction field [7].

In the previous researches, Wang et al. prepared TiO<sub>2</sub>-RGO composite *via* a single-step aerosol approach, and they also investigated the role of synthesis temperature and TiO<sub>2</sub>/GO ratio in CO<sub>2</sub> photoreduction [8]. Tu et al. developed a simultaneous reduction-hydrolysis technique to fabricate TiO<sub>2</sub>-graphene hybrid nanosheets for the reduction of CO<sub>2</sub> into CH<sub>4</sub> and C<sub>2</sub>H<sub>6</sub> [9]. Tan et al. reported a series of noble metal nanoparticles supported on reduced graphene oxide/TiO<sub>2</sub> *via* a solvothermal method, which exhibited enhanced photocatalytic activities toward the photoreduction of CO<sub>2</sub> into CH<sub>4</sub> gas [10]. Sim et al. reported rapid thermal reduced graphene oxide/Pt-TiO<sub>2</sub> nanotube arrays for enhanced photocatalytic reduction of CO<sub>2</sub> into CH<sub>4</sub> [11]. Kuai et al. achieved a CdS/reduced graphene oxide/TiO<sub>2</sub> core-shell nanostructure, which yielded greater improvements in the photoreduction of CO<sub>2</sub> [12]. Hasan et al. showed the photoelectrocatalytic reduction of CO<sub>2</sub> to CH<sub>3</sub>OH and HCOOH using a Cu-RGO-TiO<sub>2</sub> photoelectrocatalyst [13]. Xing et al. coupled boron-doped graphene nanosheets with TiO<sub>2</sub> nanoparticles for enhancing CO<sub>2</sub> photoreduction [14].

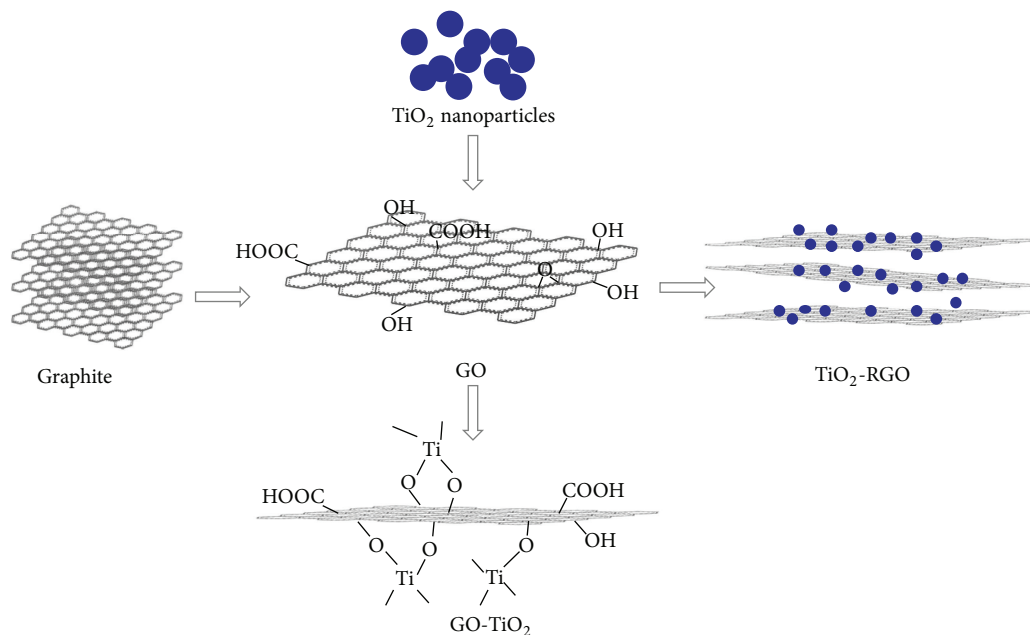


FIGURE 1: Illustration of the preparation of  $\text{TiO}_2$ -RGO nanocomposites.

Cheng et al. provided a photoelectrocatalytic technique for reduction of  $\text{CO}_2$  into chemicals [15]. Liang et al. demonstrated greater improvements in the photoreduction of  $\text{CO}_2$  by a graphene- $\text{TiO}_2$  nanocomposite with low graphene defect densities [16].

Herein, we present a simple and relatively general approach for synthesis of  $\text{TiO}_2$ -RGO nanocomposites using GO and  $\text{TiO}_2$  nanoparticles as starting materials. It is important that the procedure for preparing  $\text{TiO}_2$ -RGO nanocomposites can be carried out under ambient conditions. The high photocatalytic activity of  $\text{TiO}_2$ -RGO nanocomposites is confirmed by photocatalytic conversion of  $\text{CO}_2$  to reusable hydrocarbons ( $\text{CH}_4$  and  $\text{CH}_3\text{OH}$ ).

## 2. Experimental

**2.1. Synthesis of  $\text{TiO}_2$ -RGO Nanocomposites.** GO was prepared according to the modification of Hummers methods as described previously [17]. Typically, 0.05 g as-prepared GO dissolves in the 250 mL water in the 500 mL round-bottom flask, yielding an inhomogeneous yellow-brown dispersion. This dispersion was sonicated 20 min using an ultrasonic bath cleaner (Fisher Scientific KQ5200) until it became clear with no visible particulate matter.  $\text{TiO}_2$  nanoparticles (0.10 g) were then added into the flask, and the mixture was stirred for 24 h at room temperature. Then hydrazine monohydrate (3.00 mL, 50%) was then added to the above as-prepared product ( $\text{TiO}_2$ -GO), and the suspension was heated in an oil bath at  $100^\circ\text{C}$  under a water-cooled condenser for 24 h, where the RGO sheets gradually precipitated out as a black solid and gradually form the  $\text{TiO}_2$ -RGO. This product (Cat-2) was isolated by filtration over a medium fritted glass funnel, washed copiously with water and methanol, and dried under vacuum at  $60^\circ\text{C}$ . Cat-3 was synthesized using a similar

approach and only changed the amount of GO to 0.1 g. Pure  $\text{TiO}_2$  was marked as Cat-1.

**2.2. Materials Characterization.** The samples were characterized by Raman spectrometer (JobinYvon HR 800). Transmission electron microscope (TEM) micrographs were obtained on a Tecnai G20 (Philip) electron microscope. Brunauer-Emmett-Teller (BET) surface area of the catalysts was analyzed by  $\text{N}_2$  adsorption and desorption isotherms with a micromeritics ASAP 2020™ physisorption system. X-Ray diffraction (XRD) analysis was recorded on a XRD-6000 X-ray diffractometer (Shimadzu) with  $\text{Cu K}\alpha$  radiation ( $\lambda = 1.5406 \text{ \AA}$ ).

**2.3. Evaluation of Photocatalytic Activity.** The photocatalytic activity of the prepared  $\text{TiO}_2$ -RGO nanocomposites was studied in a double-wall cylindrical quartz reactor at ambient condition with continuous gas flow. Briefly, 0.1 g catalyst was dispersed in 100 mL distilled water containing KOH ( $0.2 \text{ mol L}^{-1}$ ). Before the reaction,  $\text{CO}_2$  was bubbled into the solution for 30 min to remove any excess air and achieve the adsorption-desorption equilibrium. High pressure mercury lamp was used as the light source (250 W).  $\text{CH}_4$  was detected as the sole product in the outlet gas based on gas chromatograph analysis. Methanol was detected by ultraviolet visible spectrophotometer.

## 3. Results and Discussion

**3.1. Characterization of  $\text{TiO}_2$ -RGO Nanocomposites.** Figure 1 shows a schematic procedure for fabricating  $\text{TiO}_2$ -RGO nanocomposites. In this straightforward procedure, GO was firstly prepared from graphite powder, followed by chemical

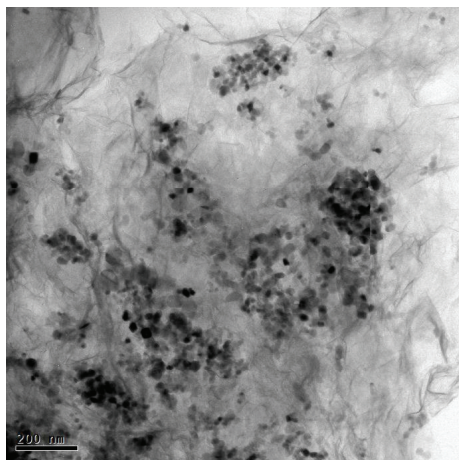


FIGURE 2: TEM image of  $\text{TiO}_2$ -RGO nanocomposites.

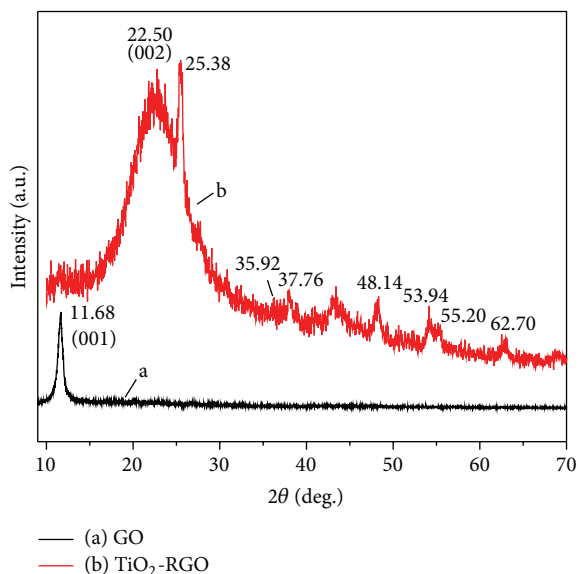


FIGURE 3: XRD patterns of (a) GO and (b)  $\text{TiO}_2$ -RGO.

deposited  $\text{TiO}_2$  nanoparticles onto GO sheet; the as-prepared materials were reduced through a hydrothermal reaction to obtain  $\text{TiO}_2$ -RGO nanocomposites.

Figure 2 shows the TEM images of the as-formed  $\text{TiO}_2$ -RGO nanocomposites. As seen from Figure 2, many nanoparticles adhered to the graphene sheets with little agglomeration, which confirms the successful immobilizing  $\text{TiO}_2$  nanoparticles on the graphene sheet. The reason for the effective assembly is that  $\text{TiO}_2$  nanoparticles can interact with functional groups such as epoxides, hydroxyl, and carboxylic acids on the GO sheets.

XRD characterization was conducted to determine the crystal structural about GO and  $\text{TiO}_2$ -RGO, and the results are shown in Figure 3. The pure GO showed a sharp peak at  $2\theta = 11.68^\circ$ , corresponding to the GO (001) plane with an interlayer spacing of 0.83 nm. It can be found that the interlayer spacing of GO is larger than that of the natural graphite powder because of the introduction of oxygen-containing

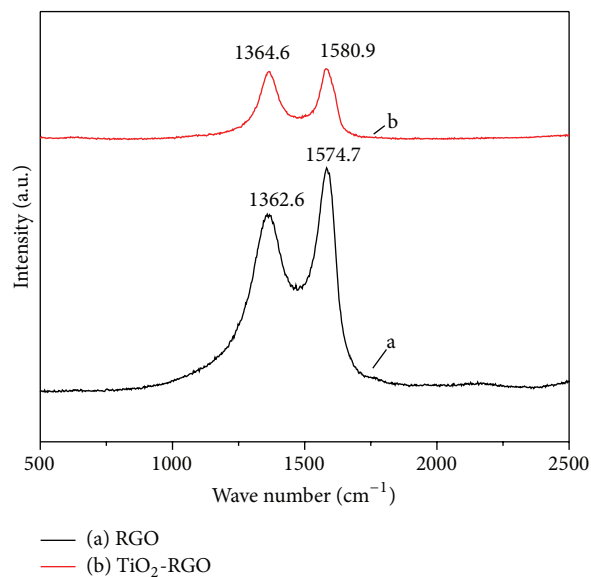


FIGURE 4: Raman spectra of (a) RGO and (b)  $\text{TiO}_2$ -RGO.

functional groups onto the surface of carbon sheet. As for  $\text{TiO}_2$ -RGO, the feature peak of the GO has disappeared and a very broad peak at  $2\theta = 22.50^\circ$ , corresponding to graphene (002) plane with an interlayer spacing of 0.40 nm, was observed, which confirms the reduction of GO to graphene in the hydrothermal environment. However, there was a small amount of residual oxygen-containing functional groups in the as-formed  $\text{TiO}_2$ -RGO nanocomposites due to the incomplete reduction of GO sheet to graphene [18]. The same phenomenon was observed in previous studies [19]. The reflection peaks at  $2\theta = 25.38, 35.92, 37.76, 48.14, 53.94, 55.20,$  and  $62.70^\circ$  can be indexed to (101), (103), (004), (200), (105), (211), and (204) crystal planes of anatase  $\text{TiO}_2$ . The XRD analysis further confirms the successful preparation of  $\text{TiO}_2$ -RGO nanocomposites.

Raman spectroscopy was utilized to examine the information about structural changes during the fabrication process. As shown in Figure 4(a), the Raman spectra of RGO exhibited a D-band peak at  $1362.6 \text{ cm}^{-1}$  and a G-band peak at  $1574.7 \text{ cm}^{-1}$ . In contrast, the G-band shifts by  $6.2 \text{ cm}^{-1}$  to a high frequency at  $1580.9 \text{ cm}^{-1}$  for  $\text{TiO}_2$ -RGO nanocomposites (Figure 4(b)), which suggests the occurrence of charge transfer between the GO sheet and  $\text{TiO}_2$  nanoparticles. It is well known that the intensity ratio of D-band to G-band ( $I_D/I_G$ ) is characteristic of the extent of disorder present within the material [20]. In our case,  $I_D/I_G$  was 0.96 for  $\text{TiO}_2$ -RGO, and it increased compared to that of the RGO ( $I_D/I_G = 0.91$ ), exhibiting a greater  $\text{sp}^2$  character. Besides, the ratio of the intensities for  $\text{TiO}_2$ -RGO is slight increased, which confirms the presence of donor molecules on graphene.

To further investigate the specific surface area of  $\text{TiO}_2$ -RGO, the  $\text{N}_2$  adsorption-desorption measurements were carried out at 77 K. Figure 5 shows that the nitrogen adsorption isotherm is a typical IV type curve. Additionally, the loop observed is ascribed as type H3 loops confirming the presence of a mesoporous structure. The specific BET surface

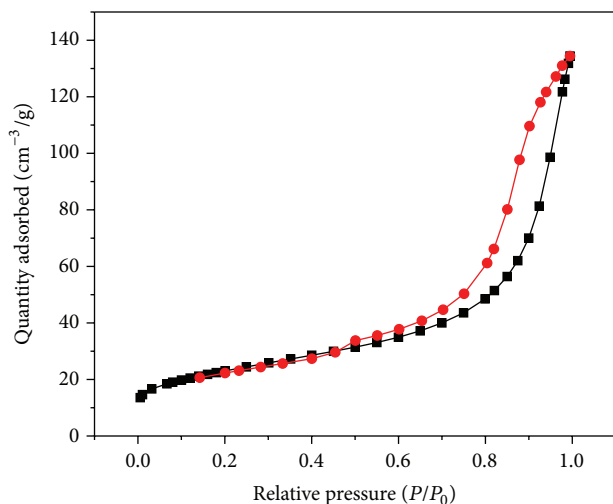


FIGURE 5: Typical nitrogen adsorption-desorption isotherm of  $\text{TiO}_2$ -RGO.

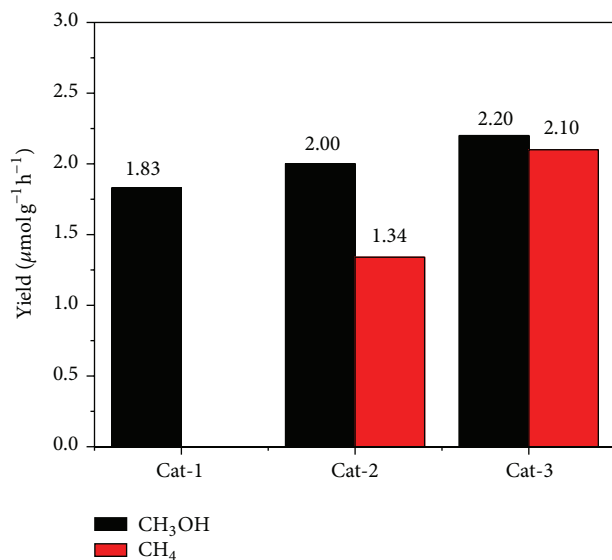


FIGURE 6: Comparison of photocatalytic activity of samples Cat-1, Cat-2, and Cat-3.

area of the as-prepared  $\text{TiO}_2$ -RGO was measured to be  $80.18 \text{ m}^2 \text{ g}^{-1}$ .

**3.2. Photocatalytic Properties of  $\text{TiO}_2$ -RGO Composites under Ultraviolet Light Irradiation.** To evaluate the photocatalytic activity of  $\text{TiO}_2$ -RGO samples, the photocatalytic  $\text{CO}_2$  conversion in the presence of KOH solution was investigated. Figure 6 shows that  $\text{CO}_2$  can be photoreduced to  $\text{CH}_3\text{OH}$  by using pure  $\text{TiO}_2$  sample (Cat-1). With the addition of graphene amount of photocatalysts,  $\text{CO}_2$  can be photoreduced to  $\text{CH}_3\text{OH}$  and  $\text{CH}_4$ . It is obvious that Cat-3 ( $2.20 \mu\text{mol g}^{-1} \text{h}^{-1}$   $\text{CH}_3\text{OH}$  and  $2.10 \mu\text{mol g}^{-1} \text{h}^{-1}$   $\text{CH}_4$ ) exhibits much higher activity than Cat-2 ( $2.0 \mu\text{mol g}^{-1} \text{h}^{-1}$   $\text{CH}_3\text{OH}$  and  $1.34 \mu\text{mol g}^{-1} \text{h}^{-1}$   $\text{CH}_4$ ). The  $\text{CH}_3\text{OH}$  yield with  $\text{TiO}_2$  was  $1.83 \mu\text{mol g}^{-1} \text{h}^{-1}$ . The results demonstrated that

the photocatalytic efficiency increased with the increases of graphene amount. With the graphene amount increased from 0 to 50%, the yields of  $\text{CH}_4$  and  $\text{CH}_3\text{OH}$  increased simultaneously. It is attributed to the increasing separation efficiency of the photogenerated electrons, because the existence of graphene could offer more active adsorption sites and photocatalytic reaction centers [21]. Furthermore, the yield efficiency increased with the increase of dispersion degree.

## 4. Conclusions

In conclusion, we present a simple and relatively general approach for synthesis of  $\text{TiO}_2$ -RGO nanocomposites under ambient conditions by using GO and  $\text{TiO}_2$  nanoparticles as starting materials. The results show that  $\text{CO}_2$  can be photoreduced to  $\text{CH}_3\text{OH}$  and  $\text{CH}_4$  by using  $\text{TiO}_2$ -RGO samples as photocatalysts. The yields of  $\text{CH}_4$  and  $\text{CH}_3\text{OH}$  can reach  $2.10 \mu\text{mol g}^{-1} \text{h}^{-1}$  and  $2.20 \mu\text{mol g}^{-1} \text{h}^{-1}$ . It is hoped that our current work could pave a way toward the fabrication of  $\text{TiO}_2$ -RGO hybrid materials and facilitate their significant applications in various fields.

## Conflict of Interests

The authors declare that there is no conflict of interests regarding the publication of this paper.

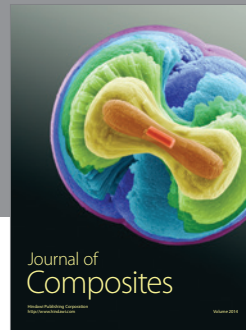
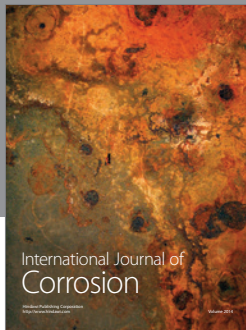
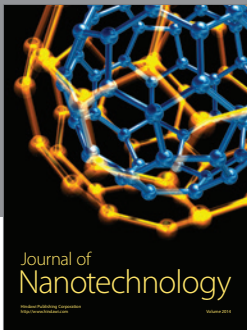
## Acknowledgment

The authors are grateful for financial support from the National Natural Science Foundation of China (Grant no. 51178142).

## References

- [1] H. Yoneyama, "Photoreduction of carbon dioxide on quantized semiconductor nanoparticles in solution," *Catalysis Today*, vol. 39, no. 3, pp. 169–175, 1997.
- [2] W. G. Tu, Y. Zhou, and Z. G. Zou, "Versatile graphene-promoting photocatalytic performance of semiconductors: basic principles, synthesis, solar energy conversion, and environmental applications," *Advanced Functional Materials*, vol. 23, no. 40, pp. 4996–5008, 2013.
- [3] A. Fujishima and K. Honda, "Electrochemical photolysis of water at a semiconductor electrode," *Nature*, vol. 238, no. 5358, pp. 37–38, 1972.
- [4] A. K. Geim and K. S. Novoselov, "The rise of graphene," *Nature Materials*, vol. 6, no. 3, pp. 183–191, 2007.
- [5] Y. Q. Sun, Q. Wu, and G. Q. Shi, "Graphene based new energy materials," *Energy & Environmental Science*, vol. 4, no. 4, pp. 1113–1132, 2011.
- [6] A. K. Geim, "Graphene: status and prospects," *Science*, vol. 324, no. 5934, pp. 1530–1534, 2009.
- [7] J. G. Low, J. G. Yu, and W. K. Ho, "Graphene-based photocatalysts for  $\text{CO}_2$  reduction to solar fuel," *The Journal of Physical Chemistry Letters*, vol. 6, no. 21, pp. 4244–4251, 2015.
- [8] W.-N. Wang, Y. Jiang, J. D. Fortner, and P. Biswas, "Nanostructured graphene-titanium dioxide composites synthesized by a single-step aerosol process for photoreduction of carbon

- dioxide,” *Environmental Engineering Science*, vol. 31, no. 7, pp. 428–434, 2014.
- [9] W. G. Tu, Y. Zhou, Q. Liu et al., “An in situ simultaneous reduction-hydrolysis technique for fabrication of TiO<sub>2</sub>-graphene 2D sandwich-like hybrid nanosheets: graphene-promoted selectivity of photocatalytic-driven hydrogenation and coupling of CO<sub>2</sub> into methane and ethane,” *Advanced Functional Materials*, vol. 23, no. 14, pp. 1743–1749, 2013.
- [10] L.-L. Tan, W.-J. Ong, S.-P. Chai, and A. R. Mohamed, “Noble metal modified reduced graphene oxide/TiO<sub>2</sub> ternary nanostructures for efficient visible-light-driven photoreduction of carbon dioxide into methane,” *Applied Catalysis B: Environmental*, vol. 166–167, pp. 251–259, 2015.
- [11] L. C. Sim, K. H. Leong, P. Saravanan, and S. Ibrahim, “Rapid thermal reduced graphene oxide/Pt–TiO<sub>2</sub> nanotube arrays for enhanced visible-light-driven photocatalytic reduction of CO<sub>2</sub>,” *Applied Surface Science*, vol. 358, pp. 122–129, 2015.
- [12] L. B. Kuai, Y. Zhou, W. G. Tu et al., “Rational construction of a CdS/reduced graphene oxide/TiO<sub>2</sub> core-shell nanostructure as an all-solid-state Z-scheme system for CO<sub>2</sub> photoreduction into solar fuels,” *RSC Advances*, vol. 5, no. 107, pp. 88409–88413, 2015.
- [13] M. R. Hasan, S. B. A. Hamid, W. J. Basirun, S. H. M. Suhaimy, and A. N. C. Mat, “A sol-gel derived, copper-doped, titanium dioxide-reduced graphene oxide nanocomposite electrode for the photoelectrocatalytic reduction of CO<sub>2</sub> to methanol and formic acid,” *RSC Advances*, vol. 5, no. 95, pp. 77803–77813, 2015.
- [14] M. Y. Xing, F. Shen, B. C. Qiu, and J. L. Zhang, “Highly-dispersed boron-doped graphene nanosheets loaded with TiO<sub>2</sub> nanoparticles for enhancing CO<sub>2</sub> photoreduction,” *Scientific Reports*, vol. 4, article 6341, 2014.
- [15] J. Cheng, M. Zhang, G. Wu, X. Wang, J. H. Zhou, and K. F. Cen, “Photoelectrocatalytic reduction of CO<sub>2</sub> into chemicals using Pt-modified reduced graphene oxide combined with Pt-modified TiO<sub>2</sub> nanotubes,” *Environmental Science & Technology*, vol. 48, no. 12, pp. 7076–7084, 2014.
- [16] Y. T. Liang, B. K. Vijayan, K. A. Gray, and M. C. Hersam, “Minimizing graphene defects enhances titania nanocomposite-based photocatalytic reduction of CO<sub>2</sub> for improved solar fuel production,” *Nano Letters*, vol. 11, no. 7, pp. 2865–2870, 2011.
- [17] W. S. Hummers Jr. and R. E. Offeman, “Preparation of graphitic oxide,” *Journal of the American Chemical Society*, vol. 80, no. 6, p. 1339, 1958.
- [18] C. Nethravathi and M. Rajamathi, “Delamination, colloidal dispersion and reassembly of alkylamine intercalated graphite oxide in alcohols,” *Carbon*, vol. 44, no. 13, pp. 2635–2641, 2006.
- [19] J. T. Zhang, Z. G. Xiong, and X. S. Zhao, “Graphene-metal-oxide composites for the degradation of dyes under visible light irradiation,” *Journal of Materials Chemistry*, vol. 21, no. 11, pp. 3634–3640, 2011.
- [20] K. N. Kudin, B. Ozbas, H. C. Schniepp, R. K. Prud’homme, I. A. Aksay, and R. Car, “Raman spectra of graphite oxide and functionalized graphene sheets,” *Nano Letters*, vol. 8, no. 1, pp. 36–41, 2008.
- [21] Q. Zhang, C.-F. Lin, B.-Y. Chen, T. Ouyang, and C.-T. Chang, “Deciphering visible light photoreductive conversion of CO<sub>2</sub> to formic acid and methanol using waste prepared material,” *Environmental Science & Technology*, vol. 49, no. 4, pp. 2405–2417, 2015.



**Hindawi**

Submit your manuscripts at  
<http://www.hindawi.com>

